Mat. Res. Soc. Symp. Vol. 635 © 2001 Materials Research Society

Strain Anisotropies in Core/Shell Magnetic Nanostructures

Georgia C. Papaefthymiou
Department of Physics, Villanova University, Villanova, PA 19085

ABSTRACT

The magnetic properties of nanosized iron-oxo molecular clusters have been investigated via Mössbauer spectroscopy and compared to those of silica coated iron-oxide nanoparticles. The clusters, prepared by controlled hydrolytic iron polymerization reactions, contain a ~ 1.2 nm diameter magnetic core of spin-coupled iron ions surrounded by a shell of benzoate ligands. The nanoparticles, prepared via sol-gel synthesis, contain a ~ 4.0 nm average diameter γ-Fe_2O_3 core coated by a shell of SiO_2. Both systems exhibit magnetic bistability at low temperatures with estimated magnetic anisotropy constants of $K_{eff} = 0.63 \times 10^5$ J/m^3 for the clusters and $K_{eff} = 0.55 \times 10^5$ J/m^3 for the particles. The similar values of K_{eff} indicate that these two systems experience similar degrees of strain at the core/shell interface. This is further supported by the values of the quadrupole splitting, ΔE_Q=0.77 mm/s for the clusters and ΔE_Q=0.75 mm/s for the particles, pointing to same degree of distortion from pure octahedral or tetrahedral symmetry at the iron coordination sites for either system. Implications of these observations for the surface atomic structure of γ-Fe_2O_3 nanoparticles are discussed.

INTRODUCTION

It has been widely observed that values of magnetic anisotropies in small particles exceed by two orders of magnitude those of their corresponding bulk magnetocrystalline anisotropies [1]. This has been attributed to the dominating effect of surface strain anisotropies in small particles. In this respect, core/shell magnetic nanostructures are of special interest as surface strain anisotropy on the magnetic core can be altered through core/shell interface microstructure manipulation. Given the important technological applications of small magnetic particles in magnetic memory storage [2] and biotechnology [3], better understanding and greater control of surface strain at the atomic level is desired.

Small core/shell particles, of ~3-10 nm diameter, are produced in finite particle size distributions leading to broad X-ray diffraction patterns. This makes detailed structural characterization of the particle core/shell interface difficult. In contrast, nanosize core/shell molecular complexes, of ~ 1-2 nm diameter, can be synthesized as monodispersed, identical, chemical structures which are amenable to X-ray structural characterization [4]. Such clusters lie at the molecular/solid boundary and exhibit collective magnetic phenomena [5]. Comparative studies of related systems may shed light at core/shell interface structural characteristics in small particles.

We have examined the electronic and magnetic properties of two iron based, nanoscale core/shell structures derived by self-assembly, co-precipitation techniques. The first structure is a nanosized iron-oxo molecular complex of the form $Fe_{16}MnO_{10}(OH)_{10}/(O_2CPh)_{20}$ [1], and the second is γ-Fe_2O_3/SiO_2 [2] nanoparticles. A comparative Mössbauer spectroscopic study of their micromagnetic properties is presented. Implications on the degree of coordination distortion of iron sites at the core/shell interface needed to produce the observed strain anisotropies of small iron-oxide magnetic particles are discussed.

MATERIALS

Iron polymerization in aqueous solutions results in the uncontrollable formation of mixtures of high molecular weight polymers. The generation of monodispersed iron-oxo nanoclusters requires competitive reaction chemistry between core cluster growth to form bulk material and cluster encapsulation by terminal ligation to arrest further core growth [5]. By using aprotic solvents as the reaction medium and adding water, needed for hydrolysis, and an organic base in limited quantities, a certain degree of control of the extent of polymerization and resulting size of the cluster can be achieved. Structurally characterized iron-oxo clusters of nuclearity Fe_3, Fe_4, Fe_6, Fe_{11} and Fe_{17} (and heterometal $Fe_{16}Mn$, $Fe_{16}Co$) have been reported [6]. Herewith, we revisit the structural and magnetic characteristics of the heterometal cluster $Fe_{16}MnO_{10}(OH)_{10}/(O_2CPh)_{20}$ [**1**] [7]. Sixteen Fe^{3+} (S=5/2) and one Mn^{2+}(S=5/2) ions superexchange-coupled through oxygen bridging ligands form a magnetic core of *ca.* 1.2 nm diameter. A surrounding shell of 20 benzoate ligands stabilizes and disperses the magnetic cores. The structure is centrosymmetric with eight unique iron crystallographic sites. See Figures 1a and b. This is a neutral molecule forming crystals through van der Waals forces.

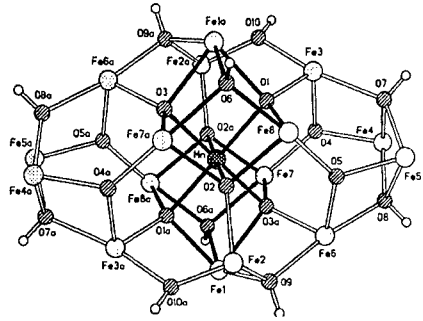

Figure 1(a). *Perspective view of the metal atoms in $Fe_{16}MnO_{10}(OH)_{10}/(O_2CPh)_{20}$ [**1**] cluster's magnetic core. Atoms are shown as spheres of arbitrary radius for clarity. Adapted from ref. [6].*

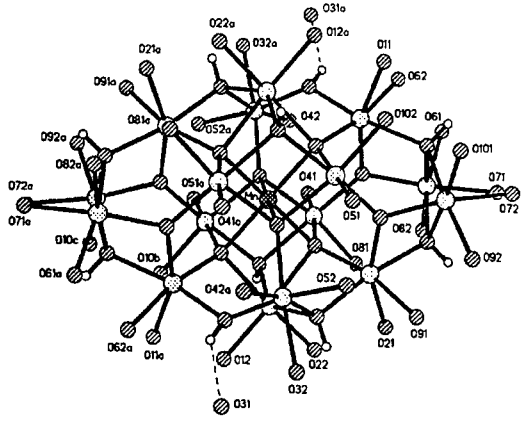

Figure 1(b). *Perspective view of metal atoms in cluster [**1**] including the iron coordinated benzoate oxygen atoms of the shell. Atoms are shown as spheres of arbitrary radius for clarity. Adapted from ref. [6].*

Bulk γ-Fe_2O_3 has a spinel structure with Fe^{3+} (S=5/2) ions situated in octahedral and tetrahedral sites. Herewith, we report on γ-Fe_2O_3 nanoparticles prepared by a sol-gel co-precipitation method, previously reported [7]. A mixture of $FeCl_2$ and $FeCl_3$ was used as starting material in order to promote crystallization of the ferrimagnetic γ-Fe_2O_3 spinel structure over the antiferromagnetic α-Fe_2O_3 structure. An inert SiO_2 coating stabilized and dispersed the particles. The γ-Fe_2O_3/SiO_2 nanocomposites were obtained as a reddish brown powder. The morphology of the magnetic particles was studied with transmission electron microscopy. TEM micrographs (Fig. 2(a), ref. [7]) indicate well-dispersed γ-Fe_2O_3 particles of average size *ca.* 4-nm diameter.

EXPERIMENTAL RESULTS

We have used Mössbauer spectroscopic methods to study the microstructural and micromagnetic properties of the [$Fe_{16}Mn$] cluster [1] and the γ-Fe_2O_3/SiO_2 particles [2]. A conventional constant acceleration Mössbauer spectrometer was used with a $^{57}Co(Rh)$ source maintained at room temperature. Sample temperatures were varied using a Lakeshore temperature controller and a Janis supervaritemp cryogenic dewar.

Mössbauer spectra of [1], cluster complex $Fe_{16}MnO_{10}(OH)_{10}/(O_2CPh)_{20}$, are shown in Figure 2. At 10 K, and higher temperatures, the spectrum is paramagnetic, with a quadrupole splitting ΔE_Q=0.77 mm/s and isomer shift δ = 0.51 mm/sec measured at 80 K, consistent with high spin S=5/2 ferric ions. At low temperatures the spectra are superparamagnetic. At 1.8 K a well defined magnetic, six-line absorption spectrum is obtained indicating that the complex has passed from fast to slow spin relaxation on the Mössbauer time scale ($\tau = 10^{-8}$ sec). A blocking temperature T_B = 4 K is estimated. The overall splitting of the magnetic spectra indicates an internal magnetic field at the iron nucleus of $\mathbf{H}_{hf}$ = 400 kOe.

Mössbauer spectra of structure [2], γ-Fe_2O_3 /SiO_2 nanoparticles are shown in Figure 3. At high temperatures the spectra are paramagnetic with ΔE_Q= 0.75 mm/s and δ = 0.43 mm/sec measured at 130 K. Below 30 K superparamagnetism is observed. Broader and noisier spectra compared to [1] are seen due to the existence of a distribution in particle-size and competing electronic absorption of the γ-ray by Si present in the sample. The saturation hyperfine field $\mathbf{H}_{hf}$ = 487 kOe and the estimated blocking temperature T_B = 23 K [7].

The observed superparamagnetism, characteristic of small magnetically ordered particles, is due to spontaneous spin reversals above their respective blocking temperatures. For magnetically isolated particles, as is the case here, the spin relaxation time is related to the average volume, V, and effective magnetic anisotropy density, K_{eff}, according to equation (1)

$$\tau_s = \tau_0 \exp (K_{eff}V/k_BT) \qquad (1)$$

where τ_0 is a constant characteristic of the material, k_B is Boltzmann's constant and T is the temperature [8]. With the Mössbauer effect, the nuclear Zeeman splitting caused by the internal magnetic field at the site of the iron nucleus is observed. However, the magnetic quantum numbers are well defined only if the Larmor precession time, τ_L, of the nuclear spin around the internal magnetic field of the particle is shorter than τ_s. The temperature at which $\tau_s = \tau_L$ defines T_B. Thus, solving for the anisotropy constant K_{eff}, equation (1) gives $K_{eff} = \ln (\tau_L / \tau_0) (k_B/V) T_B$.

K_{eff} is proportional to T_B and inversely proportional to V, the volume of the particle (or cluster). It also depends on the value of τ_0. Magnetically isolated small iron and iron-oxide particles have been measured to posses $\tau_0 \sim 10^{-9}$ to10^{-12} sec [7,9,10,11].

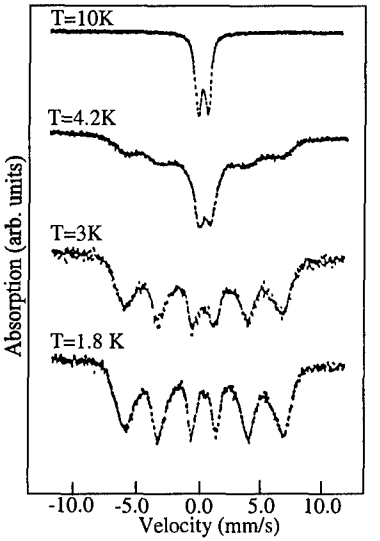

Figure 2. *Mössbauer spectra of $Fe_{16}MnO_{10}(OH)_{10}/(O_2CPh)_{20}$ at various temperatures.*

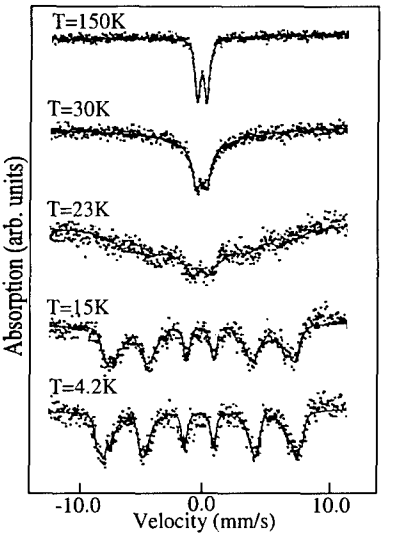

Figure 3. *Mössbauer spectra of γ-Fe_2O_3 /SiO_2 nanoparticles at various temperatures.*

Alternatively, collective magnetic excitations [12] below T_B, if observable, may be used to obtain the value of K_{eff} independently of τ_0. The manifestation of collective magnetic excitations is a temperature dependent magnetic hyperfine field below the blocking temperature which, to a first order approximation, can be described by equation (2),

$$H_{hf} = H_{hf0}\,(1-k_B T/2K_{eff}V) \qquad (2)$$

where H_{hf0} is the saturation magnetic hyperfine field at T = 0 K [12]. Detailed analysis of the temperature profile of the Mössbauer spectra for the cluster [1] and the particles [2] indicates that the iron oxide particles exhibit collective magnetic excitations below their blocking temperature, while those of the cluster do not.

Analysis of collective magnetic excitation processes below T_B for the γ-Fe_2O_3 /SiO_2 nanoparticles determined K_{eff} and τ_0 to be: $K_{eff} = 0.55 \times 10^5$ J/m^3 and $\tau_0 = 3.3 \times 10^{-11}$ sec [7]. The anisotropy constant for the cluster was determined from its blocking temperature to be: $K_{eff} = 0.66 \times 10^5$ J/m^3, assuming $\tau_0 \sim 10^{-9}$ sec [13]. The observed values of K_{eff} are two orders of magnitude larger than the magnetocrystalline anisotropy of epitaxial single-crystal films and polycrystalline powders of γ-Fe_2O_3 ($K_{mc} = 4.7 \times 10^3$ J/m^3) [14,15].

The effective anisotropy constant is given by $K_{eff} = K_{mc} + K_{sh} + K_s + K_\sigma$, where K_{mc} is the magnetocrystalline anisotropy of the material, K_{sh} is the shape anisotropy of the particle, K_s the surface anisotropy, and K_σ the strain anisotropy [16]. For spherical core/shell nanostructures the strain at the interface is the most significant contribution, making the K_σ term the most dominant.

In bulk γ-Fe_2O_3, Fe^{3+} ions occupy octahedral or tetrahedral sites of a spinel structure, and exhibit no quadrupole splitting. The observed non-vanishing ΔE_Q in small particles of γ-Fe_2O_3 is associated with crystallographic distortions away from perfect octahedral or tetrahedral iron coordination symmetry, due to lattice strain at the particle core/shell interface. The degree of distortion must correlate with the magnitude of strain contributions to K_{eff}. No structural characterization of the core/shell interface is possible, however, in small particles, due to size distributions rendering broadened X-ray absorption spectra.

In contrast, detailed X-ray structural information of cluster [**1**] is possible, and has been obtained (Figures 1a and b). All iron ions are octahedrally coordinated to oxygen atoms. Iron-oxygen bonds pointing either into the interior of the core, along its surface or outwardly towards the benzoate ligands of the shell are clearly discernible. Selected O-Fe-O bond angles have been tabulated in Table I. Due to space limitations only the angles along the x, y and z coordinates of local octahedra are tabulated. The complete set of bond angles and bond lengths is available in the supplementary material of ref. [6].

Table I. Selected O-Fe-O bond angles in degrees for the [$Fe_{16}Mn$] cluster of Figure 1(a) and (b). The structure is centrosymmetric with only eight unique iron crystallographic sites. Corresponding O-Mn-O angles are also included for comparison. Complete set of bond angles and bond lengths are given in the supplementary materials of ref. [6].

O(9)-Fe(1) -O(6a)	145.2	O(7)-Fe(4)-O(82)	170.4	O(41)-Fe(7)-O(3a)	173.8
O(22)-Fe(1)-O(1a)	169.5	O(4)-Fe(4)-O(71)	169.8	O(5)-Fe(8)-O(6)	169.1
O(12)-Fe(1)-O(3a)	175.8	O(8)-Fe(5)-O(101)	171.1	O(2)-Fe(8)-O(102)	168.6
O(2)-Fe(2)-O(32)	173.8	O(5)-Fe(5)-O(72)	167.7	O(1)-Fe(8)-O(51)	173.8
O(52)-Fe(2)-O(10a)	170.5	O(7)-Fe(5)-O(92)	170.4	O(3)-Mn-O(3a)	180.0
O(9)-Fe(2)-O(42a)	169.2	O(5)-Fe(6)-O(21)	159.0	O(1)-Mn-O(3)	180.0
O(1)-Fe(3)-O(62a)	169.2	O(8)-Fe(6)-O(9)	170.9	O(2)-Mn-O(2a)	180.0
O(7)-Fe(3)-O(10)	166.3	O(91)-Fe(6)-O(3a)	164.8		
O(4)-Fe(3)-O(11)	159.4	O(4)-Fe(7)-O(6a)	170.1		
O(8)-Fe(4)-O(61)	165.0	O(81)-Fe(7)-O(2a)	168.2		

The greatest distortion is associated with Fe (1) with 9.16% deviation from 180 degrees. expected for perfect octahedral coordination. The smallest distortion is exhibited by Fe (2) with 4.91% deviation. The average deviation for all 8 unique iron crystallographic sites is 6.67%. The central Mn ion possesses perfect octahedral oxygen coordination. The observed distortions produce unresolved, non-vanishing quadrupole splittings at the iron sites of an average value $\Delta E_Q = 0.77$ mm/sec measured at 80 K, and create shear stress at the surface of the magnetic core resulting in the observed $K_{eff} = 0.63 \times 10^5$ J/m^3.

The comparable values of ΔE_Q and K_{eff} measured for structures [1] and [2], would indicate that bond angles at the core/shell interface of the γ-Fe_2O_3 particles must be similarly distorted relative to the bulk spinel structure (ignoring, for simplicity, contributions of bond-length distortions). Thus, large strains of the order of 6% to 7% may be structurally imposed at the core/shell interface resulting in magnetic surface reconstruction, spin canting [17,18], high shear stresses and a value of K_{eff} of the order of 10^5 J/m^3 for the γ-Fe_2O_3 /SiO_2 nanoparticles. It is noteworthy that this observed strain is two to three orders of magnitude larger than the magnetostriction constant of bulk polycrystalline γ-Fe_2O_3 ($\lambda = 2.2 \times 10^{-5}$) [19].

CONCLUSION

It is well established that nanosized particles of iron-oxide and iron-hydroxide phases exhibit non-vanishing quadrupole splittings and magnetic anisotropy constants of the order of 10^5 J/m^3. It is also well established that the magnetic anisotropies are sensitive to surface modifications. Lacking detailed structural information of the core/shell interface in most nanoparticulate systems, the degree of surface strain structurally imposed is unknown. We have proposed that nanosized, structurally characterized iron-oxo molecular clusters exhibiting comparable K_{eff} and ΔE_Q values model the microstructure of the core/shell interface in small iron oxide magnetic particles. This has led to the proposition that structurally imposed strains at the surface of *ca.* 4nm diameter silica-coated iron-oxide particles may be of the order of several percent.

ACKNOWLEDGMENTS

The author is indebted to Professors S. Lippard and J. Ying of MIT, in whose laboratories structures [1] and [2], respectively, were synthesized. The author wishes to thank Dr. Arthur Viescas for technical support and Dr. John Vassiliou for useful discussions. She also thanks the National Science Foundation for financial support, under contract number DMR-0074537.

REFERENCES

1. *Magnetic Properties of Fine Particles,* J. Dorman and D. Fiorani Eds. (North-Holland 1991).
2. A.E. Berkowitz, F.T. Parker, F.E. Spada and D. Margulies, *ibid,* p.309.
3. *Scientific and Clinical Applications of Magnetic Carriers,* ed. by U. Häfeli, W. Schütt, J. Teller and Zborowski (Plenum, New York, 1997).
4. G. C. Papaefthymiou, *Hyperfine Interactions,* **113**, 357, (1998) and references there in.
5. G. C. Papaefthymiou, *Phys. Rev. B*, **46**, 10366 (1992).
6. W. Micklitz, V. Mckee, R. Lyn Rardin, L. E. Pence, G.C. Papaefthymiou, S.G. Bott and S.J. Lippard, *J. Am. Chem. Soc.* **116**, 8061 (1994).
7. L. Zhang, G.C. Papaefthymiou and J.Y. Ying, *J. Appl. Phys.* **81**, 6892 (1997).
8. W.F. Brown Jr., *Phys. Rev.,* **130**, 1677 (1963).
9. B.H. Sohn, R.E. Cohen and G.C. Papaefthymiou, *J. Mag. Mag. Mat.* **182**, 216 (1998).
10. C.L. Chien, in: *Science and Technology of Nanostructured Magnetic Materials*, G.C. Hadjipanayis, G.A. Prinz Eds., NATO ASI Series B, **259** (Plenum Press, N.Y. 1991) p. 4772
11. D.P.E. Dickson, N.M.Reid, C. Hunt, H.D. Williams, M.E. Hilo and K. O' Grandy, *J. Mag. Mag. Mat.,* **125**, 345 (1993).
12. S. Mørup and H. Topsøe, *J. Appl. Phys.* **11**, 63 (1976).
13. G.C. Papaefthymiou, *Mat. Res. Soc. Symp. Proc.* **286**, (1993) p. 67.
14. H. Takei and S. Shiba, *J. Phys. Soc. Jpn.,* **21**, 1255 (1966).
15. A.H. Morrish and E.P. Valstyn, *J. Phys. Soc. Jpn.*, **17 B-1**, 392 (1962).
16. A.H. Morrish, *The Physical Principles of Magnetism* (John Wiley & Sons, New York, 1965).
17. J.M.D. Coey, *Phys. Rev. Lett.,* **17,** 1140 (1971).
18. R.H. Kadama, A.E. Berkowitz, E.J. McNiff, Jr. and S. Foner, *Phys. Rev. Lett.*, **77**, 394 (1996)
19. V.A.M. Brabers in: *Handbook of Magnetic Materials,* K.H.J. Buschow Ed. (Elsevier, Amsterdam, 1995), vol. **8**, p. 189.

Metallic Nanowires